

Anticancer Activity of Iso-Mukaadial Acetate on Pancreatic and Colon Cancer Cells

Portia Raphela-Choma*¹, Lesetja Motadi¹,
Mthokosizi Simelane¹, Mpho Choene¹

Abstract

Background: Pancreatic cancer and colon cancer pose significant challenges in treatment, with poor prognoses. Natural products have long been explored for their potential as anticancer agents. Iso-mukaadial acetate has shown promise in inducing apoptosis in breast and ovarian cancer cells. The objective of this study was to investigate the effect of Iso-mukaadial acetate on pancreatic (MIA-PACA2) and colon (HT29) cancer cell lines.

Methods: Pancreatic (MIA-PACA2) cancer cells, colon (HT29) cancer cells, normal embryonic kidney cells (HEK 293), and normal lung cells (MRC5) were cultured and treated with Iso-mukaadial acetate (IMA) for 24 hours. The viability assays were conducted using Alamarblue reagent and a real-time cell viability monitoring system, xCELLigence. The IC₅₀ values were determined, followed by assessments of ATP production, caspase 3/7 activation, mitochondrial function, morphological changes using a light microscope, and gene expression changes via RT-PCR.

Results: This study indicates that Iso-mukaadial acetate exhibited concentration-dependent cytotoxic effects, slowing cellular proliferation in both cancer cell lines. Activation of the mitochondrial apoptotic pathway and caspase 3/7 suggests induction of apoptosis. Reduced ATP production and altered gene expression further support its anticancer properties. Morphological changes after treatment with Iso-mukaadial acetate showed apoptotic characteristics which may suggest that apoptosis was induced.

Conclusion: According to the results obtained, Iso-mukaadial acetate shows potential as an anticancer agent, evidenced by its effects on cellular viability, mitochondrial function, ATP production, caspase activation, and gene expression in pancreatic and colon cancer cells. These findings highlight its promise for further investigation and potential in the development of therapeutic agents.

Keywords: Anticancer, Colon cancer, Iso-mukaadial acetate, Natural products, Pancreatic cancer.

Introduction

Pancreatic cancer, is one of the resistant cancers to cancer therapies with a poor prognosis has one of the lowest survival rates, with fewer than five years (1). Colon cancer, ranked as the third most life-threatening cancer globally, presents high incidences in both genders, with less than a five-year survival rate for metastatic cases (2,3). Natural products, long explored for novel and

safer anticancer agents (4), offer advantages such as efficacy and reduced toxicity, especially to normal cells (5). Criteria for potential agents include being natural, easily obtainable, highly selective, safe, cost-effective, soluble, and specific (6). Identifying an agent with all these qualities remains challenging but crucial for cancer patients (7). Improved treatment strategies

1: Department of Biochemistry, University of Johannesburg, Corner Kingsway and University Road, Auckland Park, Johannesburg, 2092, South Africa.

**Corresponding author: Portia Raphela-Choma; Tel: +27 839774576; E-mail: portiaapheladi22@gmail.com.*

Received: 19 Jun, 2023; Accepted: 7 Apr, 2024

could lower mortality and incidence rates, while enhanced screening and diagnostic technologies could aid in early cancer detection (8).

Iso-mukaadial acetate (IMA), a natural compound from *Warbugia salutaris* bark, belongs to the drimane sesquiterpenoid class. Previous studies have highlighted its antimalarial, anti-diabetic, and anticancer properties (9-11). This study aims to elucidate IMA's mechanism of action and its potential anticancer activity in pancreatic (MIA-PACA2) and colon (HT29) cancer cells.

Pancreatic cancer, known for its resistance to therapies and poor prognosis, has one of the lowest survival rates, with fewer than five years (1). Colon cancer, ranked as the third most life-threatening cancer globally, presents high incidences in both genders, with less than a five-year survival rate for metastatic cases (2,3). Natural products, long explored for novel and safer anticancer agents (4), offer advantages such as efficacy and reduced toxicity, especially to normal cells (5). Criteria for potential agents include being natural, easily obtainable, highly selective, safe, cost-effective, soluble, and specific (6). Identifying an agent with all these qualities remains challenging but crucial for cancer patients (7). Improved treatment strategies could lower mortality and incidence rates, while enhanced screening and diagnostic technologies could aid in early cancer detection (8).

Iso-mukaadial acetate (IMA), a natural compound from *Warbugia salutaris* bark, belongs to the drimane sesquiterpenoid class. Previous studies have highlighted its antimalarial, anti-diabetic, and anticancer properties (9-11). This study aims to elucidate IMA's mechanism of action and its potential anticancer activity in pancreatic (MIA-PACA2) and colon (HT29) cancer cells.

Materials and Methods

Materials

Iso-mukaadial acetate (IMA) was previously isolated from *Warbugia Salutaris* stem bark at the University of KwaZulu Natal. DMEM

media (Gibco), 10% fetal bovine serum (Gibco), penicillin-streptomycin (Gibco), and amphotericin B (Gibco) were purchased from Thermo Fischer. HEK293, donated by Dr. Engelbrecht Z University of Witwatersrand, SA), MRC5 donated by colleagues in the University of Pretoria, SA. MIA-PACA2 and HT29 cell lines were purchased from ATCC, USA. DPBS (HyClone), 1X trypsin-EDTA (Gibco), and Alamarblue (Invitrogen) were purchased from Thermo Fischer. Trypan Blue (0.4%) (LONZA) was purchased from White Sci. Caspase-Glo® 3/7 assay, Relia-Prep RNA cell miniprep kit, mitochondrial ToxGlo™ kit, and CellTiter-Glo® 2.0 Reagent kit were purchased at Promega. DMSO was purchased from Monitoring and Control Laboratories (MCL). The cells, HEK 293, MRC5, MIA-PACA2, and HT29 cell lines (ATCC) were cultured in DMEM media (Gibco), 10% fetal bovine serum (Gibco), 1% penicillin-streptomycin (Thermo Fischer Scientific, Gibco), and 1% amphotericin B (Gibco). The viability of the cells was measured by 0.4% Trypan blue solution (LONZA, WhiteSci).

Cytotoxicity test using AlamarBlue Reagent

A stock concentration of 10 mM of (IMA) was prepared and dissolved in a 100 % sterile-filtered cell culture grade DMSO. After preparation, the stock was kept at 4 °C until use.

In order to achieve the requisite confluency for experiments, the normal embryonic kidney cells (HEK 293), and normal lung cells (MRC5), and MIA-PACA2, and HT29 cancer cell lines were grown to the required size (70-80 % confluency). These cells were grown in DMEM supplemented with 10 % fetal bovine serum, 1 % penicillin-streptomycin, and 1% amphotericin B. For all cell lines, 1.0×10^5 cells/well were employed at a final volume of 100 µl in each well of 96-well plates, which were then incubated for 24 hours. After incubation, the following IMA concentrations were applied: 12.5 µM, 6.25 µM, 3.125 µM, 1.56 µM, and 0.78 µM. Cells from normal and cancer cell lines were treated with these concentrations. A 200 mg/ml concentration of

cisplatin was utilized as a positive control. Cells were treated as a blank and with DMSO (0.1%) as a negative control. Following a 24-hour treatment period, alamarblue (10 μ l) was added. The mixture was then incubated for 2 hours and examined using a fluorescent microplate reader (Synergy HT, Agilent?).

Real-time cell viability analysis using the xCELLigence system

Before use, the xCELLigence equipment was put in an incubator and calibrated. Cell lines MIA-PACA2, HT29, MRC5, and HEK 293 were seeded on the E16 well plates for 24 hours (1 x 10⁵ cells/ml). After 24 hours, the cell lines were given the same IMA concentrations as alamarblue and allowed to run for 3 days. The positive control was cisplatin (200 g/ml), whereas the negative control was DMSO (0.1%). The RTCA system tracked the RTCA's performance and documented its findings.

Caspase 3/7 assay

Following the identification of the IC₅₀ values of IMA for both pancreatic and colon cancer cells, the activity of caspase 3/7 in the MIA-PACA2 and HT-29 cell lines was assessed using the Caspase-Glo® 3/7 assay kit. The 96 well microplates were used to culture and seed the MIA-PACA2 (2 x 10⁵) and HT-29 (2 x 10⁵) cell lines for 24 hours. Following treatment, the wells were filled with the caspase-Glo® reagent, which was then incubated for 20 to 30 minutes on the shaker. The luciferase activity was measured and shown as Relative Luminescence Units using a luminescence microplate reader (Synergy HT, Agilent).

Mitochondrial Membrane Potential assay

The mitochondrial integrity of the MIA-PACA2 and HT29 cell lines after treatment with IMA was measured using the Promega mitochondrial ToxGlo™ kit following the manufacturer's instructions. Before use, the bis-AAF-R110 substrate and cytotoxicity test buffer were frozen in a water bath at 37 °C. 2 ml of assay buffer and bis-AAF-R110 substrate were combined after thawing. In 96-

well microplates, MIA-PACA2 (2 x 10⁵) and HT-29 (2 x 10⁵) cell lines were seeded for 24 hours before being treated for 24 hours. Following treatment, 100 μ l of the ToxGlo reagent was added to each well, and they were shaken for 30 minutes. Microplate reader (Synergy HT) fluorescence was used to evaluate the mitochondrial activity.

Cellular ATP assay

The ATP synthesis in the MIA-PACA2 and HT29 cell lines following treatment with IMA was measured using the CellTiter-Glo® 2.0 Reagent kit following the manufacturer's instructions from Promega. The HT-29 (2 x 10⁵) and MIA-PACA2 (2 x 10⁵) cell lines were treated for 24 hours after being plated in 96-well microplates for 24 hours. The reagent was added to the wells (100 μ l) and shaken for 10 minutes after treatment after defrosting at room temperature. The ATP activity was calculated using a microplate reader (Synergy HT) and luminescence.

Morphological analysis using a Light microscope

MIA-PACA2 and HT 29 cancer cells were plated in petri dishes for 24 hours, then treated with IMA IC₅₀ concentrations after 24 hours of seeding. Morphological changes to confirm apoptosis were observed and captured after 24 hours of treatment using light microscopy.

Extraction of RNA using Relia-Prep™ RNA-cell miniprep kit

Cells from the MIA-PACA2 and HT29 cell lines were harvested before cell lysis, and after being centrifuged at 300 x g for five minutes, the cells were collected in an Eppendorf tube. After microcentrifugation at a speed of 300 x g for 5 minutes, DPBS was used to wash the cells. After removing the supernatant, 100 μ l of the BL-TG Buffer mixture was poured into the pellets and vortexed. The mixture was combined with 35 μ l of isopropanol and vortexed for 5 seconds. Cell lysates were placed into a Minicolumn and centrifuged at 13,000 x g for 30 seconds in a microcentrifuge.

The Minicolumn was filled with 500 µl of RNA wash solution, and it was centrifuged for 30 seconds at 13,000 x g. Each Minicolumn tube received 30 l of prepared DNase I, and the combination was incubated at room temperature for 15 minutes. Following the incubation, 200 µl of column wash solution was added, and for 15 seconds, the sample was centrifuged at 13,000 x g. After adding the RNA wash solution, the sample mixture was microcentrifuged for two minutes at its maximum speed. The sample mixture was microcentrifuged once more for 1 minute at a speed of 13,000 x g. The purity of the RNA collected from both cell lines was measured using Nano-Drop, which allowed us to quantify the isolated RNA. RNA was kept at -80 °C until it was needed.

Gene expression analysis of Iso-mukaadial acetate

The genes tested for expression before and after treatment were TP53 (ID: 7157); CDKN1A (ID: 1026); CDK2 (ID: 1017); RBBP6 (ID: 5930); BAX (ID: 581); BCL2 (ID: 596); GAPDH (ID: 2597) and Beta Actin (ID: 11461). Primers, random primers, and RNA templates were used in combination. The sample combination was promptly refrigerated on ice for 5 minutes after being incubated at 70 °C for 5 minutes in a heat block. The combination was immediately added to the reverse transcription mixture and refrigerated on ice after being vortexed for 10 seconds. After starting, the cDNA synthesis was kept at -80 °C for later use. The final gene expression analysis was performed by combining the iTaq™ Universal SYBR® Green Supermix, primers, and cDNA. Real-time PCR was performed on a CFX96-connect system.

Isolation and characterization of natural Iso-mukaadial acetate

To selectively obtain an IMA fraction, dichloromethane was used to extract the compounds before isolating IMA. - Semi-preparative liquid chromatography with a C18 stationary phase allowed for the separation of

80 fractions, which were analyzed by LC-HRMS. The material obtained was sufficient for a full characterization by 1H and 13C NMR to confirm the identity of the compound.

Statistical analysis

Graph Pad Prism, xCELLigence system, and Light microscope were used to analyze the results. Data was communicated as mean ± Standard Deviation (*P <0.05, **P <0.01 ***P <0.001). A p-value less than 0.05 (p <0.05) was deemed significant.

Results

The cytotoxicity assay showed that IMA had a concentration-dependent cytotoxic effect on all cell lines (Figs. 1 & 2).

Caspase 3/7 was shown to be activated in both cancer cell lines. A decrease in mitochondrial membrane potential (MMP) was observed with a decrease in ATP generation, after treatment with IMA (Figs. 3 & 4). Exposure of IMA to MIA-PACA2 and HT29 cancer cells showed apoptotic features such as cell shrinkage or rounding, membrane blebbing, and losing contact with other nearby cells and apoptotic bodies (Fig. 5). The same characteristics were observed after treatment with cisplatin. Cell detachment was also observed which could be a sign of early apoptosis as observed.

The expression of selected genes associated with cell cycle arrest and apoptosis induction showed (Figs. 6 & 7), in MIA-PACA2 cells p53 was downregulated and was upregulated in HT29 cells. In both cancer cell lines, where Bax (pro-apoptotic gene) was highly upregulated in comparison to the upregulation of the Bcl2 gene. P21 was significantly upregulated in both cancer cell lines while RBBP6 and CDK2 were downregulated after treatment with IMA in MIA-PACA2. RBBP6 was upregulated in HT29 and CDK2 was downregulated after treatment with IMA in HT29 cells. The chemical identification of IMA and their unambiguous 1H and 13C assignments were achieved by NMR spectroscopy.

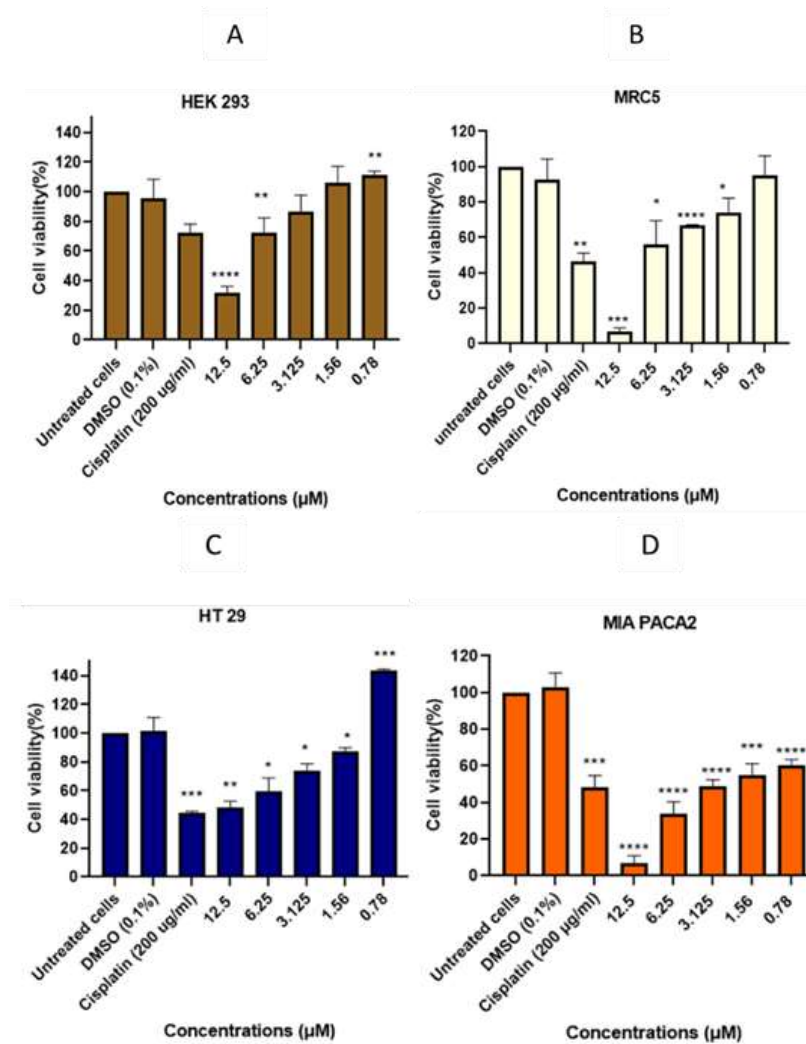


Fig. 1. Morphological changes in MIA-PACA2 and HT29 cell line. The endpoint assay used to determine the cytotoxic effects of IMA on the cell lines MIA-PACA2, HT-29, HEK 293, and MRC5. The data from three biological replicates were expressed as mean Standard Deviation (* $P < 0.05$, ** $P < 0.01$, *** $P < 0.001$, **** $P < 0.0001$).

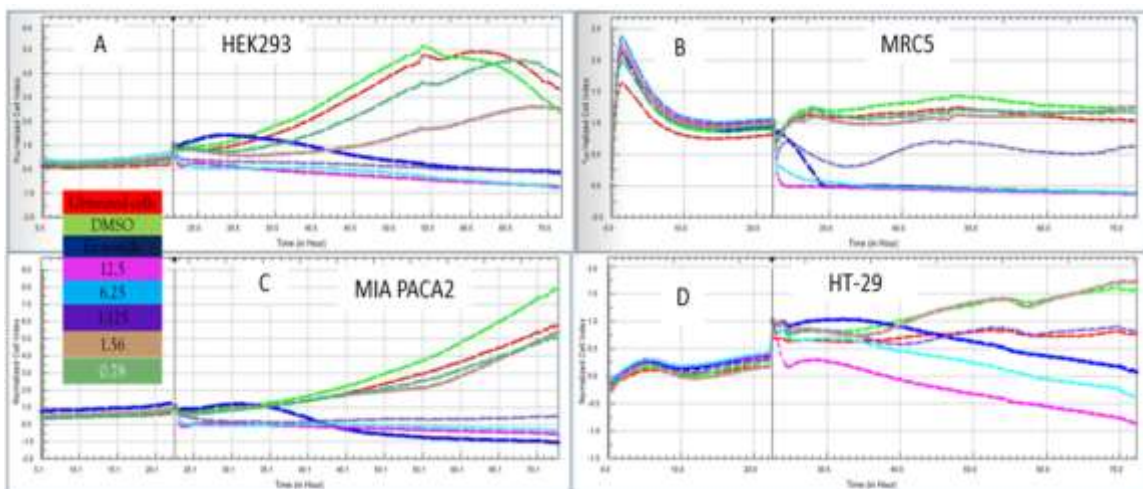


Fig. 2. Cytotoxic effect of IMA using Real-Time Cell Analyzer (xCELLigence) on HEK 293, MRC5 MIA-PACA2, and HT29, cell lines. Cytotoxic impact of IMA utilizing RTCA (over 48 hours) on the MIA-PACA2, HT-29, HEK 293, and MRC5 cell lines.

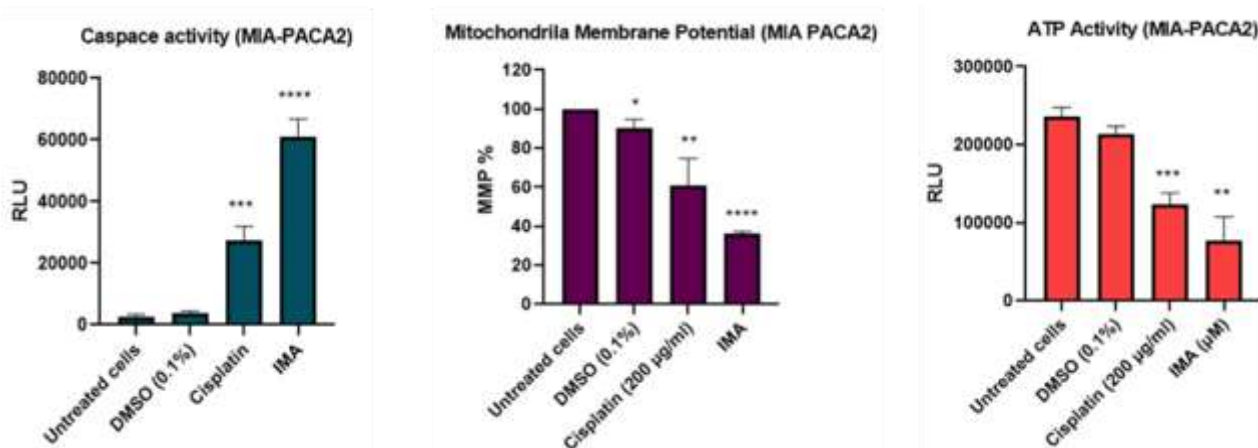


Fig. 3. Activation of caspase 3/7, MMP integrity and ATP activity on MIA-PACA2 cell line. Caspase 3/7 activation, MMP and ATP controlled by the bioactive of IMA on MIA PACA2 cell lines. The cells were treated with IMA IC50 (2.4 µM) for 24 hours. The data were expressed as mean ± Standard Deviation (*P< 0.05, **P< 0.01 ***P< 0.001, ****P< 0.0001) from three biological repeats.

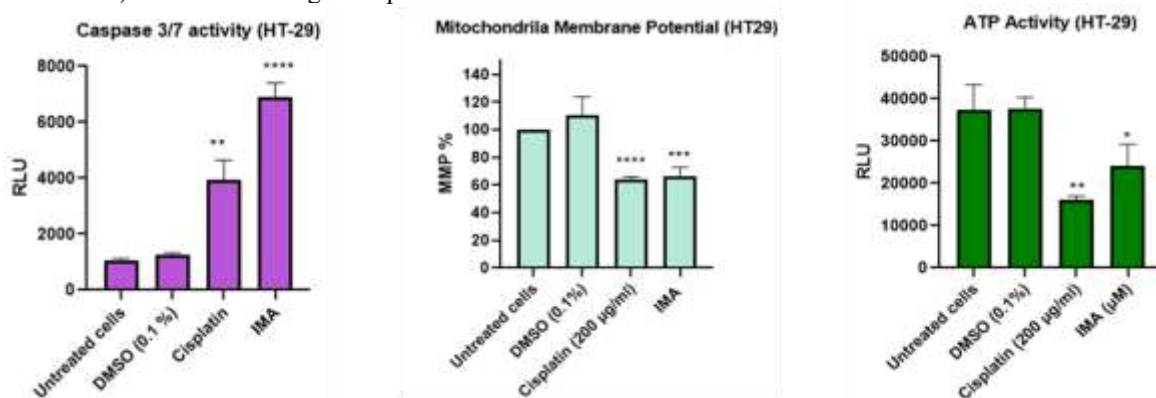


Fig. 4. IMA triggered caspase 3/7 activation of caspase 3/7, MMP dysfunction and ATP activity in HT29 cell line. Caspase 3/7 activation, MMP and ATP regulated by the bioactive of IMA on HT29 cell lines. The cells were treated with IMA IC50 (12.2 µM) for 24 hours. The data were expressed as mean ± Standard Deviation (*P< 0.05, **P< 0.01 ***P< 0.001, ****P< 0.0001) from three biological repeats.

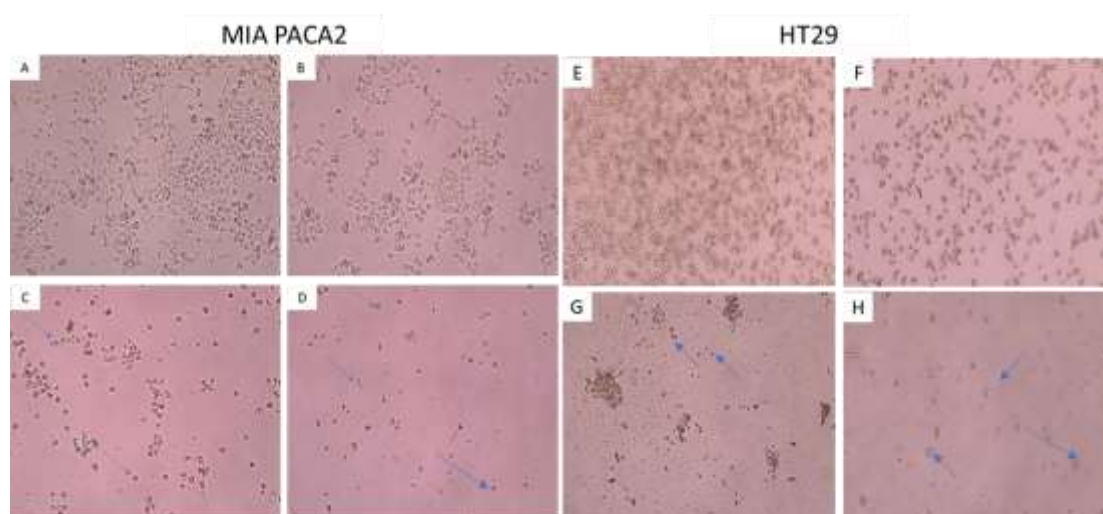


Fig. 5. Morphological changes in MIA-PACA2 and HT29 cell line. MIA-PACA2 and HT29 cell lines displayed distinct morphological changes after treatment with IMA for 24 hours. Untreated cells represented by (A, E), DMSO (0.1 %) (B, F), Cisplatin 200 µg/ml (C, G), and IMA (2.4 µM, 12.2 µM) (D, H).

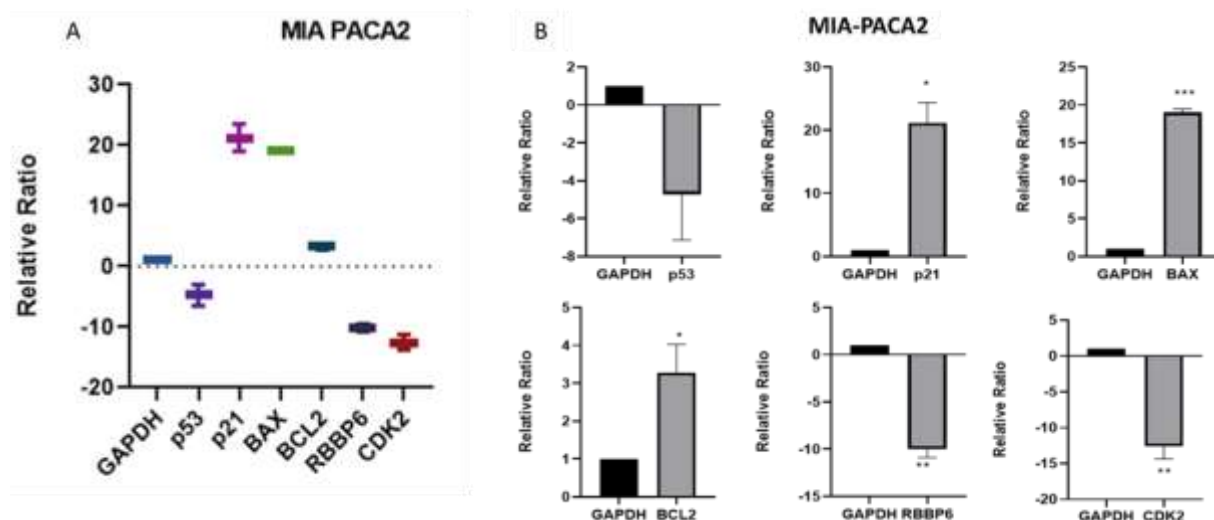


Fig. 6. Gene expression using real-time PCR in MIA-PACA2 cell line. Results were analyzed by the comparative C(T) method and GraphPad prism. The following box plots (A) represent MIA-PACA2 cell line gene expression after a 24-hour treatment with IMA. GAPDH was used as a reference gene. The data were expressed as mean \pm Standard Deviation from two biological repeats (* $P < 0.05$, ** $P < 0.01$, *** $P < 0.001$).

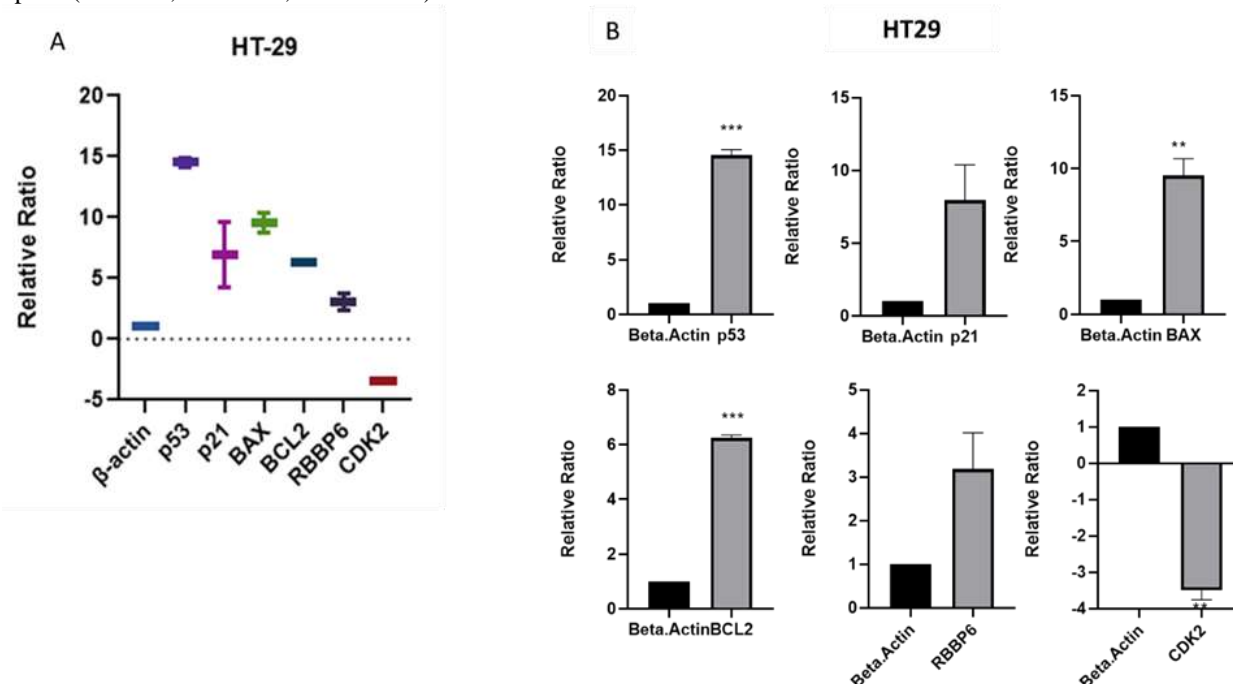


Fig. 7. Gene expression using real-time PCR in HT29 cell line. Real-time PCR results were analyzed comparative C(T) method and GraphPad prism. (A) represent HT29 cell line gene expression after a 24-hour treatment with IMA. Beta-actin was used as reference genes. The data were expressed as mean \pm Standard Deviation from two biological repeats (* $P < 0.05$, ** $P < 0.01$, *** $P < 0.001$).

Discussion

Our study revealed that at high concentrations, IMA demonstrated toxicity towards both normal and cancer cells, whereas at lower concentrations, its toxicity was more pronounced towards cancer cells, exhibiting a concentration and cell-type-dependent pattern. IMA is a very potent compound and the time

of IMA exposure to the cells plays a critical role in determining how effective it is. The type of cell line also plays a critical role in how cells respond to the toxicity of compounds. To determine the potential anticancer mechanism induced by IMA on MIA-PACA2 and HT29 cancer cells, caspase 3/7 activity, MMP

integrity, ATP activity, and gene expression were evaluated.

Caspases are important activators in the induction of programmed cell death (apoptosis) due to the disruption of mitochondria in cells (12). Mitochondria were disrupted in MIA-PACA2 and HT29 cells after treatment with IMA which signals that cytochrome C was released to elicit the activation of initiator caspases that lead to the induction of apoptosis by effector caspase 3/7 proteases. This was also supported by the decrease in cellular ATP production in both cancer cells after treatment which suggested that there was less activity in the mitochondria as a result of cell death. Programmed cell death (apoptosis) is also associated with morphological changes which were observed in both cancer cells after treatment with IMA such as cell shrinkage/rounding and membrane blebbing. In a previous study, pancreatic cancer cells showed a decrease in MMP after treatment with tomentosin (8). The decrease in MMP in pancreatic cancer cells after IMA treatment showed that mitochondria-mediated intrinsic pathways may have been induced. Another previous study showed that after treatment cellular ATP was decreased in pancreatic cancer cells, hence, induction of apoptosis was observed (1). Previously, MMP levels were decreased in colon cancer cells after treatment, which shows that there was mitochondrial dysfunction and possible apoptotic induction.

The dysfunction of cell cycle phases in cancers contributes to the over-proliferation of cells. In the cell cycle, each phase is well controlled by cyclin-dependent kinases as they allow the cell to move from one phase to another. Upregulation of p21 inhibits the activity of CDKs in the cell cycle by causing cell cycle arrest (13). After treatment with IMA in MIA-PACA2 and HT29 cancer cells, p21 was upregulated and CDK2 was downregulated. This shows that IMA may have possibly arrested cells during the cell cycle however a cell cycle test would have been necessary to test the idea. It is reported that the activation of p21 can be mediated by

p53, or a p53-independent pathway as observed in this study, p53 was upregulated in MIA-PACA2 cells and downregulated in HT29 cells after treatment with IMA. The same observations were recorded when IMA was treated on breast and ovarian cancer cells. P53-independent pathways result in an apoptotic response (12). It was reported that colon cancer cells have been marked as p53 mutants and that did not affect the activation of p21 (13), after treatment with IMA, as it is p53-independent. The induction of mitochondrial apoptosis can be triggered by DNA damage, cellular stress, or overproduction of reactive oxygen species. The dysfunction of mitochondria can elicit the activation of pro-apoptotic members. When Bax (pro-apoptotic members) are expressed in higher amounts, they block the expression of Bcl2 members (anti-apoptotic members) to allow the cells to undergo apoptosis (14). After treatment with IMA in both cancer cells, Bax/Bcl2 ratio was observed. Bax was highly expressed in MIA-PACA2 and HT29 cells and the reduction in Bcl2 expression was observed in both cancers. These observations suggested that the mechanism of cellular death after treatment with IMA may be a mitochondria-mediated intrinsic pathway. Bax/Bcl2 ratio expression was also observed in breast cancer (MDA-MB 231) and ovarian cancer (RMG-1) cancer cells treated with IMA (12). Previous studies showed that after treatment Bax/Bcl2 expression ratio was observed in pancreatic cancer cells which may signal that apoptosis was induced (13). RBBP6 was expressed in HT29 cancer cells and downregulated in MIA-PACA2 cells. RBBP6 is a protein that binds to p53 to inhibit its activity, and this may lead to a delay in apoptosis and cell proliferation (15). In this study, the expression level of p53 was higher than the expression level of RBBP6 in HT29 cells. IMA is a purely natural product that was initially found by Prof Semilane and colleagues from the University of KwaZulu Natal and has previously been shown to have anti-proliferative properties in breast and ovarian cancer cell lines (12).

This study showed that the modification of the mitochondrial intrinsic route may be a potential mechanism of action for the cytotoxic effect of IMA on pancreatic (MIA- PACA2) and colon (HT29) cancer cells. MMP disruption, caspase 3/7 activation, and cellular ATP decrease are all correlated with Bax/Bcl2 expression. According to the data, IMA might be a promising agent for colon and pancreatic cancer cells, though it is quite potent. Examination of protein expression, cell cycle arrest, and other genes/proteins involved in preventing cancer growth need to be

researched in the future.

Acknowledgments

The authors would like to give thanks to everyone who contributed to the study financially and with the necessary equipment.

Conflict of interest

No conflict of interest.

Funding

National Research Foundation (NRF) and Thuthuka (TTK).

References

- Atlı Şekeroğlu Z, Şekeroğlu V, Işık S, Aydın B. Trimetazidine alone or in combination with gemcitabine and/or abraxanedecreased cell viability, migration and ATP levels and induced apoptosis of human pancreatic cells. *Clin Res Hepatol Gastroenterol.* 2021;45(6):101632.
- Ghodousi-Dehnavi E, Arjmand M, Akbari Z, Aminzadeh M, Haji Hosseini R. Anti-Cancer Effect of Dorema Ammoniacum Gum by Targeting Metabolic Reprogramming by Regulating APC, P53, KRAS Gene Expression in HT-29 Human Colon Cancer Cells. *Rep Biochem Mol Biol.* 2023;12(1):127-135.
- Shalmashi H, Safaei S, Shanebandi D, Asadi M, Bornehdeli S, Mehdi Navaz A. Evaluation of lncRNA FOXD2-AS1 Expression as a Diagnostic Biomarker in Colorectal Cancer. *Rep Biochem Mol Biol.* 2022;11(3):471-478.
- Yu J, Zhong B, Xiao Q, Du L, Hou Y, Sun HS, et al. Induction of programmed necrosis: A novel anti-cancer strategy for natural compounds. *Pharmacol Ther.* 2020;214:107593.
- Zeng A, Hua H, Liu L, Zhao J. Betulinic acid induces apoptosis and inhibits metastasis of human colorectal cancer cells in vitro and in vivo. *Bioorg Med Chem.* 2019;27(12):2546-2552.
- Ginsburg H, Deharo E. A call for using natural compounds in the development of new antimalarial treatments - an introduction. *Malar J.* 2011;10:S1.
- Majolo F, Delwing LKDOB, Marmitt DJ, Bustamante-Filho IC, Goettert MI. Medicinal plants and bioactive natural compounds for cancer treatment: Important advances for drug discovery. *Phytochem Lett.* 2019;31:196-207.
- Miura K, Satoh M, Kinouchi M, Yamamoto K, Hasegawa Y, Kakugawa Y, et al. The use of natural products in colorectal cancer drug discovery. *Expert Opin Drug Discov.* 2015;10(4):411-26.
- Lkhagvasuren K, Kim JK. Ziyuglycoside II induces caspases-dependent and caspases-independent apoptosis in human colon cancer cells. *Toxicol In Vitro.* 2019;59:255-262.
- Güçlü E, Çınar Ayan İ, Dursun HG, Vural H. Tomentosin induces apoptosis in pancreatic cancer cells through increasing reactive oxygen species and decreasing mitochondrial membrane potential. *Toxicol In Vitro.* 2022;84:105458.
- Msomi NZ, Shode FO, Poe OJ, Mazibuko-Mbeje S, Simelane MBC. Iso-Mukaadial Acetate from Warburgia salutaris Enhances Glucose Uptake in the L6 Rat Myoblast Cell Line. *Biomolecules.* 2019;9(10):520.

12. Raphela-Choma PP, Simelane MBC, Choene MS. Evaluation of the antiproliferative effect of Iso-mukaadial acetate on breast and ovarian cancer cells. *Adv Tradit Med.* 2023;23:251-260.

13. Nyaba ZN, Murambiwa P, Opoku AR, Mukaratirwa S, Shode FO, Simelane MBC. Isolation, characterization, and biological evaluation of a potent anti-malarial drimane sesquiterpene from *Warburgia salutaris* stem bark. *Malar J.* 2018;17(1):296.

14. Aamazadeh F, Ostadrahimi A, Rahbar Saadat Y, Barar J. Bitter apricot ethanolic extract induces apoptosis through increasing expression of Bax/Bcl-2 ratio and caspase-3 in PANC-1 pancreatic cancer cells. *Mol Biol Rep.* 2020;47(3):1895-1904.

15. Dlamini Z, Ledwaba T, Hull R, Naicker S, Mbita Z. RBBP6 Is Abundantly Expressed in Human Cervical Carcinoma and May Be Implicated in Its Malignant Progression. *Biomark Cancer.* 2019;11:1179299X19829149.